

## Monitoring Vegetation Change Using Forest Cover Density Model

Windi Tri Andini<sup>1</sup>, Nurlina<sup>1\*</sup>, Ichsan Ridwan<sup>1</sup>

<sup>1</sup> Physics Study Program, Mathematics and Natural Sciences Faculty, Universitas Lambung Mangkurat. Jl. Ahmad Yani Km. 36 Banjarbaru, Kalimantan Selatan, Indonesia

\* Corresponding author's e-mail: [nurlina\\_abdullah@ulm.ac.id](mailto:nurlina_abdullah@ulm.ac.id)

### ABSTRACT

The regional ecological environment has become a significant subject of study due to the dynamics of the ecosystem, which is represented by vegetation, under the influence of human activities. The objective of this research is to demonstrate the implementation and effectiveness of the forest canopy density (FCD) model in generating a map that illustrates changes in forest canopy density using multitemporal remote sensing data in Tabunio watershed. The methodology relies on vegetation index, including the normalized difference vegetation index (NDVI), shadow index (SI), and bare soil index (BI), to generate a composite vegetation index (CVI). FCD uses multitemporal remote sensing data from Landsat TM images from 2005 to 2020, which have been utilized to accomplish multi-source categorization. The findings indicated that the vegetation coverage of the Tabunio watershed presented a predominant pattern of high coverage in the northeastern and eastern regions, whereas most areas of the western region had low coverage; (2) vegetation cover from 2005 to 2020 is dominated by sparse to very dense vegetation cover classes; (3) changes in vegetation cover over two decades are very significant. The expansion of plantation land in 2005 caused a lot of non-vegetated land, which gradually changed in the following year period along with plant growth. At the end of 2020, the percentage of very dense vegetation became increasingly dominant, which was around 42 percent. The results of the study indicate the three biophysical index (NDVI, SI, and BI) used in this model approach were appropriate for precisely discriminating across all canopy density classes, as seen by the overall producer's accuracy of 81.3%. FCD model in multitemporal data can help in the early identification of deforestation or forest degradation activities. Furthermore, the FCD model may have certain constraints, as it requires an understanding of ground conditions to establish threshold values for each class.

**Keywords:** forest cover density, change detection, multitemporal, Tabunio Watershed.

### INTRODUCTION

Vegetation makes up the primary element of terrestrial ecology, which plays a crucial role in energy exchange, water cycle, and biogeochemical cycles [Y. Song et al., 2018]. The transfer of matter and energy between the pedosphere and atmosphere is contingent upon vegetation [Long et al., 2021]. Vegetation change has been and will remain a critical concern in the context of global changes that impact terrestrial ecosystems due to its susceptibility to climate change [Ben Abbes et al., 2018; Richards & Belcher, 2020]. W. Song et al., [2017] noted that in numerous ecological scenarios, it may be necessary to map a variety of

vegetation cover types over extensive geographical regions at regular intervals, given the variability of these conditions over seasons and years. The conventional evaluation condition of the vegetation is based on a variety of Systematic sampling methods that may be difficult to get across a large expanse and to update in a timely manner [Ejegu et al., 2022]. The utilization of open source spatial data has significantly enhanced research on land cover change, as a result of the development of geospatial device and the improvement of the approach of vegetation mapping. This has enabled an precision assessment of the health and distribution of the world's agricultural, grassland, and forest resources, a matter that has emerged as a critical

concern in the realm of environmental sustainability [Baloloy et al., 2020]. In recent years, the utilization of remote sensing image (spatial data) has been of significant assistance in the monitoring of the evolving vegetation pattern. The expanding availability of remote-sensed data at different geographical, spectral, and temporal resolutions offers the opportunity to observe the biophysical attributes of ecological systems across different terrain sizes [Ben Abbes et al., 2018; Huylensbroeck et al., 2020; Richards & Belcher, 2020; Sun et al., 2021]. The researchers have shown that temporal remotely sensed data can be used to monitor efficiently, precisely and analyze the spatiotemporal dynamics of vegetation cover.

Various image classification methods have been created to facilitate the quantitative and qualitative evaluation of forest vegetation using remotely sensed data. [Guha & Govil, 2021; Li et al., 2014; Mu et al., 2018; Y. Song et al., 2018]. Remote sensing data can be used to determine forest parameters such density, species characteristics, volume, biomass, leaf area index, canopy density, and canopy cover [Clevers et al., 2017; Fang et al., 2021; Ghosh et al., 2021; Sahana et al., 2015; W. Song et al., 2017]. There are differences in vegetation cover density estimation, mainly due to differences in remote sensing data, vegetation indices and classification algorithms. Previous studies have often used a single vegetation index or algorithm to map and analyze vegetation density, such as NDVI, SAVI, EVI, RVI, GNDVI and NDWI [Gao et al., 2020]. NDVI is one of the most popular vegetation index for mapping vegetation density, but NDVI is sensitive to atmospheric and lighting conditions, affected by the presence of clouds and shadows and less effective for detecting vegetation in areas with very low or very high vegetation cover [Huang et al., 2021; Carbajal-Morán et al., 2023]. SAVI, requires adjustment of parameter L for various soil conditions, which can be complicated, is also still affected by atmospheric conditions although better than NDVI [Gupta et al., 2018]. EVI more complex in its calculations than NDVI, calibration parameters G, C1, C2, and L require adjustment and are also affected by soil moisture and canopy structure [Samanta et al., 2021]. Whereas RVI is susceptible to saturation at very high or low values [Yan et al., 2022]. Overall, a single vegetation index typically uses two or three spectral bands (e.g. NDVI uses red and near infrared band), which can lead to limitations in identifying

different land cover types or different vegetation conditions. It is often very sensitive to disturbances such as clouds, shadows, and soil moisture, for example, NDVI can be affected by the presence of clouds or high moisture in the soil, resulting in lower classification accuracy in separating different vegetation types or land conditions due to limited spectral information. A single vegetation index may be less effective in distinguishing between vegetation types that have similar spectral characteristics. And most importantly, it has difficulty in overcoming the seasonal variability of vegetation because it uses little spectral information. Thus, although single vegetation indices are easy to calculate and use, they have limitations in terms of accuracy, sensitivity to disturbance, and discrimination ability compared to more sophisticated composite vegetation indices (Aires et al., 2020; Amiri et al., 2009; Jia et al., 2019; Mazzarino & Finn, 2016; Ouyang et al., 2010; Tian et al., 2021; Vaghela et al., 2018). with some of the shortcomings of the single vegetation index mentioned above, this study tries to use a composite index to map vegetation cover in the Tabunio watershed. it is expected that this composite index will improve the accuracy of mapping vegetation cover density. As we know, vegetation mapping often becomes less accurate due to the reflection effect of bare soil (Li et al., 2014). This is evidenced by the positive correlation between vegetation cover with NDVI and shadow index (SI), and a negative correlation with bare soil index (BI) [Godinho et al., 2016]. The combination of the three index is known as the forest canopy density (FCD) model. Until now, the FCD model has rarely made changes, especially to the vegetation index indicators. Different from another FCD model that often used advanced vegetation index (AVI) [Loi et al., 2017; Nugraha & Citra, 2020], this study use NDVI to replace the frequently used vegetation index, combine with shadow index (SI) and bare soil index (BI). According to several studies, to map vegetation cover comparing the AVI, EVI, SAVI and NDVI vegetation index mostly provide the results of using the NDVI vegetation index with higher accuracy, especially for the classification of vegetation density in the tropics [Durigon et al., 2014; Gandhi et al., 2015; Huang et al., 2021; Hussain & Islam, 2020; Mazzarino & Finn, 2016; Zaitunah et al., 2018]. In addition, another novelty of this research is that tries to apply the FCD model for monitoring vegetation change using multitemporal satellite data.

The condition of the Tabunio Watershed as a watershed with priority handling [Decree of the Minister of Forestry No. SK. 328/Menhut-II/2009] because the criterion for extremely high recovery includes the state of essential land, which has a total area of 19,109.89 hectares. Likewise, the condition of vegetation cover and erosion index qualify as very high recovery with erosion of 219.08 tonnes ha<sup>-1</sup> year<sup>-1</sup>. Additionally, the deteriorated water catchment conditions led to drought all along the dry season and flood during the rainy season. The environmental destruction in the Tabunio watershed is worsened by the existence of conventional gold mining, which has become a cause for worry for multiple stakeholders. It is imperative to assess the biophysical characteristics of the Tabunio watershed in light of the escalating frequency of natural disasters, including droughts, landslides, and flooding [Ridwan et al., 2024; Wibawa et al., 2021]. Few of the studies in Tabunio Watershed in the past have been focused to classify land use and land cover type [Nurlina et al., 2021], to assess soil erosion [Kadir et al., 2016; Nurlina et al., 2022] and critical land [Auliana et al., 2018; Nurlina et al., 2023]. Thus far, the result has been utilized to accurately measure the sustainability of time series data. However, it has not yet been utilized for predicting vegetation

change in the Tabunio Watershed. In the description above, the objective of this research is to showcase the application and effectiveness of the FCD model in generating a map that illustrates alterations in forest canopy density. This will be achieved by utilizing multitemporal remote sensing data in the Tabunio Watershed. It's necessary to examine the condition of vegetation cover with spatial and temporal distribution in the Tabunio watershed during the previous twenty years.

### METHODS

The research site is situated in the Tabunio Watershed, which spans an area of 62,558.56 hectares in Tanah Laut Regency. It is situated at 114°36'12.02"–114°57'47.62" East and 3°37'2.72"–3°51' 51.43" LS. The Tabunio watershed is administratively divided into 44 localities, 6 sub-districts, and 10 sub-watersheds. The map depicting the investigation location of the Tabunio watershed and the area of each sub-watershed is shown in Figure 1.

The FCD mapping model is an analyze method used to calculate vegetation cover density by using and integrating index related to forest vegetation cover index [Loi et al., 2017]. The

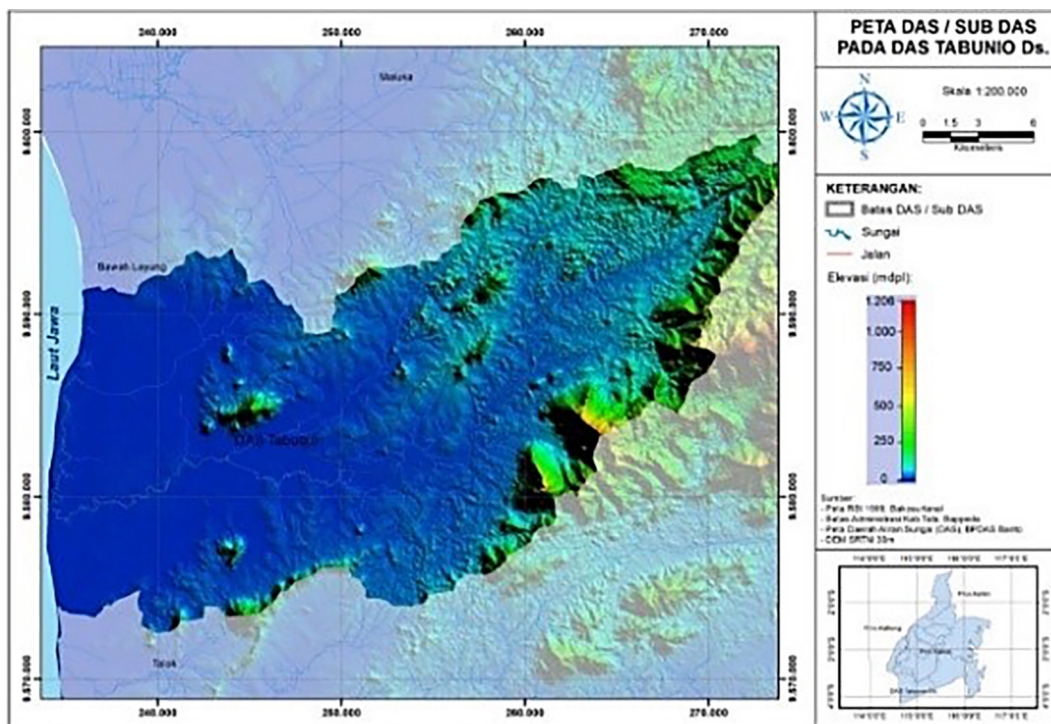


Figure 1. Map of Tabunio watershed research location

methodology relies on vegetation indices, including the normalized difference vegetation index (NDVI), shadow index (SI), and bare soil index (BI), to create the composite vegetation index (CVI). The FCD model indicates that there is a positive correlation between vegetation cover and both SI and NDVI, but there is a negative correlation between vegetation cover and BI. Hence, the integration of NDVI, BI, and SI can be employed to form CVI, so mitigating the impact of shadow and background soil. [Clevers *et al.*, 2017].

$$CVI = (NDVI + nBI) \times SI \quad (1)$$

where:  $n$  – the harmonic coefficient, can take values between -1 and 0.

Through meticulous testing in this scientific field, it has been shown that a value of  $n = -0.05$  yields acceptable outcomes. The pixel dichotomy approach was employed to quantify the extent of vegetation coverage.

$$VC = \frac{(CVI - CVI_{soil})}{(CVI_{veg} - CVI_{soil})} \quad (2)$$

where:  $CVI_{veg}$  and  $CVI_{soil}$  are the CVI values of vegetation and bare soil cover.

$$NDVI = \frac{\rho_{NIR} - \rho_{RED}}{\rho_{NIR} + \rho_{RED}} \quad NDVI = \frac{\rho_{NIR} - \rho_{RED}}{\rho_{NIR} + \rho_{RED}} \quad (3)$$

$$SI = \left[ \frac{(256 - \rho_{BLUE}) \times (256 - \rho_{GREEN}) \times (256 - \rho_{red})}{\times (256 - \rho_{GREEN}) \times (256 - \rho_{red})} \right]^{1/3} \quad (4)$$

$$BI = \frac{\rho_{swir} + \rho_{RED} - \rho_{NIR} - \rho_{BLUE}}{\rho_{swir} + \rho_{RED} + \rho_{NIR} + \rho_{BLUE}} \quad (5)$$

where:  $\rho_{BLUE}$ ,  $\rho_{GREEN}$ ,  $\rho_{RED}$ ,  $\rho_{NIR}$ , and  $\rho_{SWIR}$  represent the reflectance of the Landsat image in the blue, green, red, near infrared and first shortwave infrared bands, respectively.

The combination of *bands* selected is 543 to produce true colors. The use of *band* four and *band* three as NDVI transformation is because, At these specific wavelengths, there is a significant

disparity in the way objects are reflected on vegetation and dirt, making it sound like an estimator of the vegetation density model [Guo *et al.*, 2022]. The processing results in NDVI values that can be classified based on the range of NDVI values ranging from -1 non-vegetation to +1 (vegetation). Image analysis for vegetation density interpretation uses digital analysis that groups pixels into classes based on reflectance values. Then classified into several vegetation density classes ranging from sparse to dense vegetation (Table 1).

The accuracy of image classifications is typically evaluated using kappa coefficient and confusion matrix [Nurlina *et al.*, 2021]. To assess the accuracy of FCD model, a confusion matrix was created. From this matrix, four accuracy assessment metrics were calculated: overall classification accuracy (OA), producer’s accuracy (PA), user’s accuracy (UA), and Kappa coefficient (K). The effectiveness of the FCD model in predicting forest canopy density was subsequently validated by a study of the derived accuracy measures.

## RESULTS AND DISCUSSION

The map in Figure 2 was analyzed for the period 2005–2020 using Equation 3. The analysis shows that the NDVI decreased throughout the duration of the study, although the NDVI of 2005–2010 was generally higher than that of the following 2 periods. Temperature and precipitation exert varying influences on NDVI across different spatial and temporal domains. The variance in NDVI in most sections of the Tabunio watershed is mostly influenced by temperature and rainfall.

The annual SI values for 2005–2020 are shown in Figure 3, respectively. As seen in the figure, SI values and distribution vary. In vegetated areas, SI varies with plant cover type. In the Tabunio watershed, there are coniferous forests, broadleaf forests, oil palm plantations, rubber, shrubs, and agricultural land in SI values arranged in decreasing order. SI also varies with canopy structure, such as broadleaf, closed, or open canopy. Therefore, SI proves valuable for conducting in-depth vegetation study, including the categorization of different vegetation kinds and gaining insights into the current state of plant growth.

In the Figure 4 according to this map, the proportion of land covered by each level of canopy density varies between 2005 and 2020. The FCD model analysis showed that the high-density

**Table 1.** Vegetation density class and NDVI index values [Aires *et al.*, 2020]

Vegetation density level	Vegetation index value
Non-vegetation	< 0.1
Rare	0.10–0.2
Medium	0.21–0.40
Meetings	0.41–0.60
Very tight	>0.6

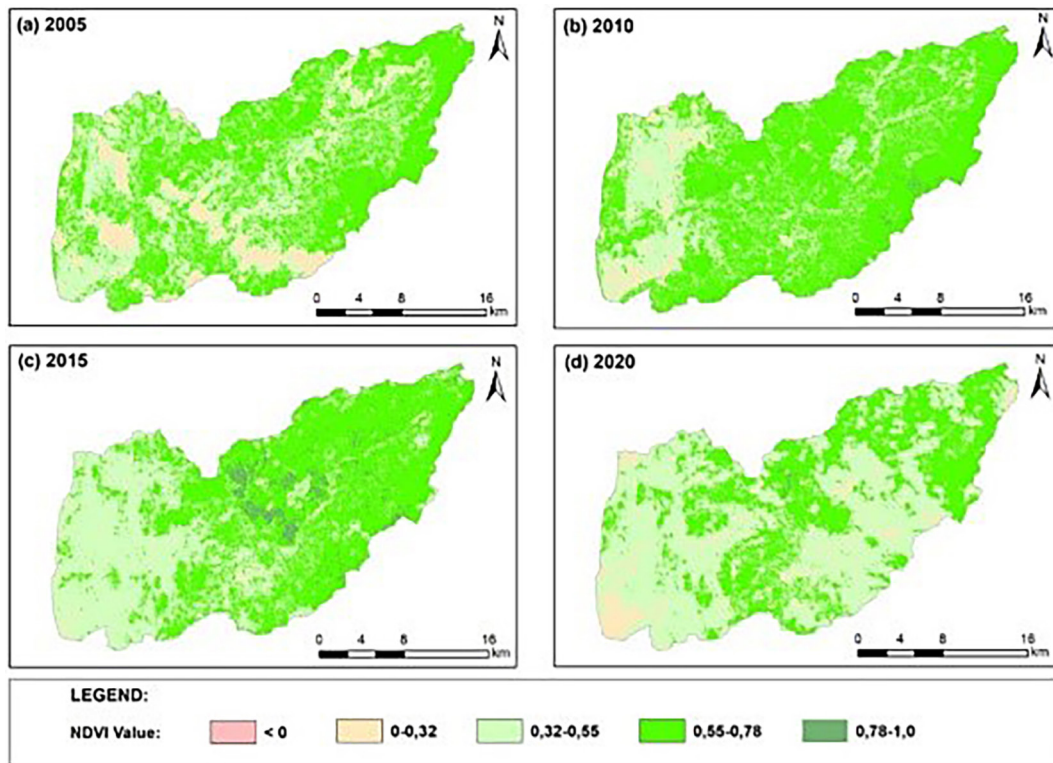


Figure 2. Normalized difference vegetation index [NDVI] of Tabunio Watershed 2005–2020

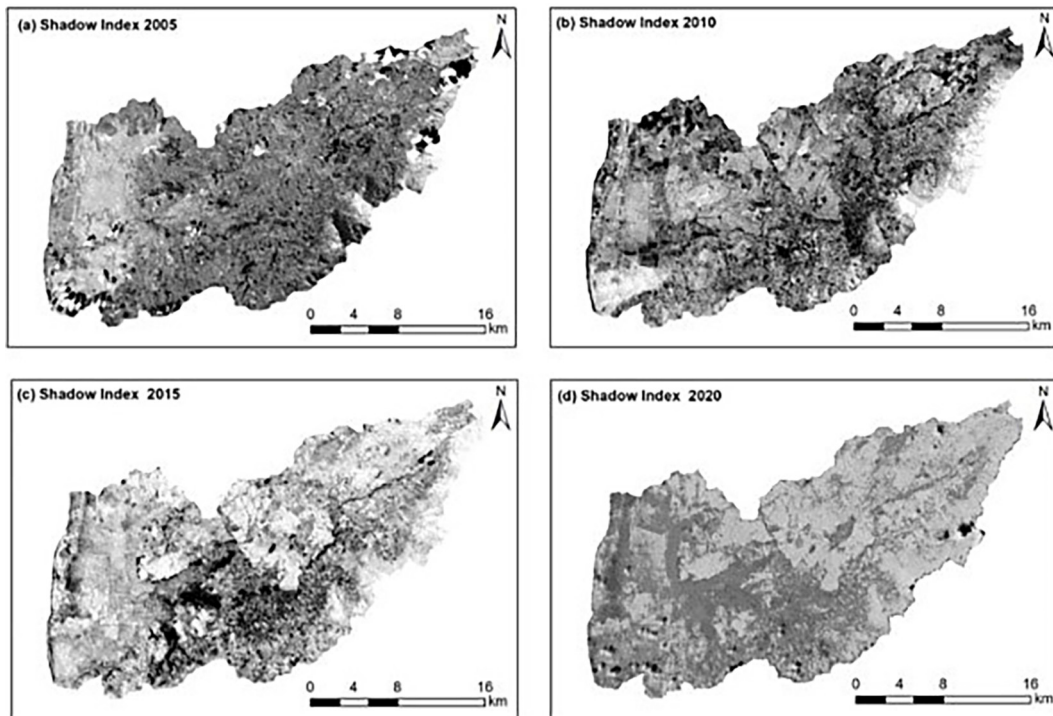


Figure 3. Shadow index of Tabunio watershed 2005–2020

class is the most dominant, covering 41.9% of the entire Tabunio watershed area, followed by the medium-density class and the sparse vegetation class, which occupied 22.24 and 15.71%,

respectively. The Results table derived from using the FCD model demonstrates a decline in the ratio of the area across low to high-density categories. Hence, the outcomes achieved suggest

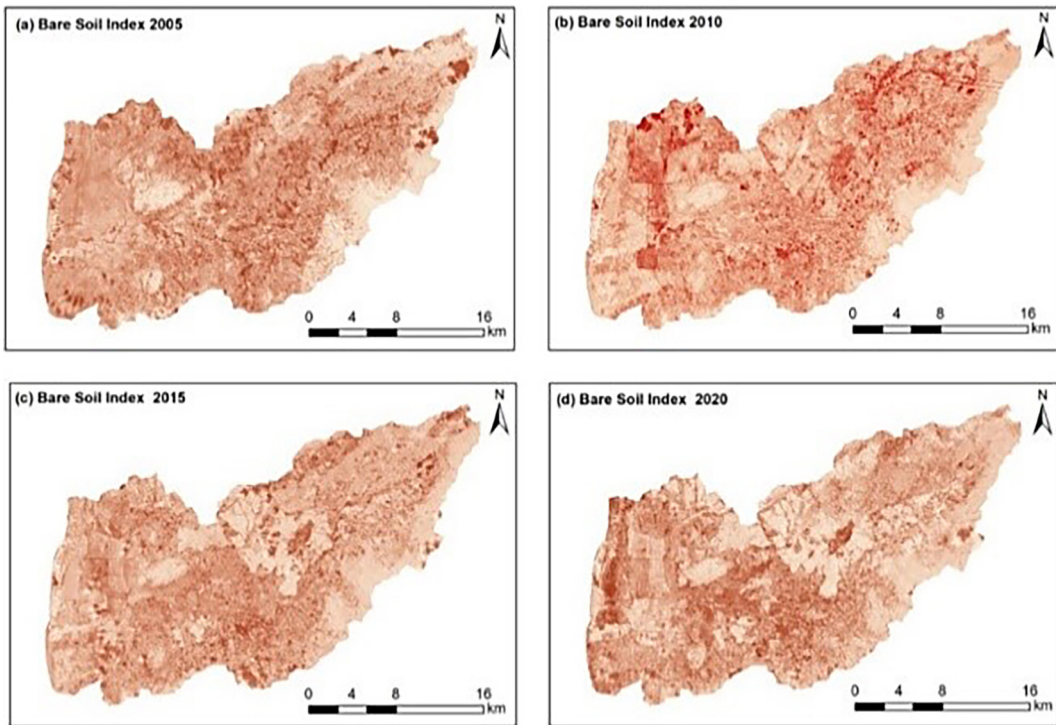


Figure 4. Spatial distribution of bare soil index in Tabunio Watershed 2005–2020

that the dependability of the FCD model remains unaffected by the area, as it consistently demonstrates the same pattern (with low-density classes occupying a greater proportion of the space compared to medium and high-density classes).

The state of vegetation coverage in the Tabunio watershed between 2005 and 2020 is dominated by sparse to very dense vegetation cover classes (Fig. 5). Changes in vegetation cover over 20 years are very significant. The expansion

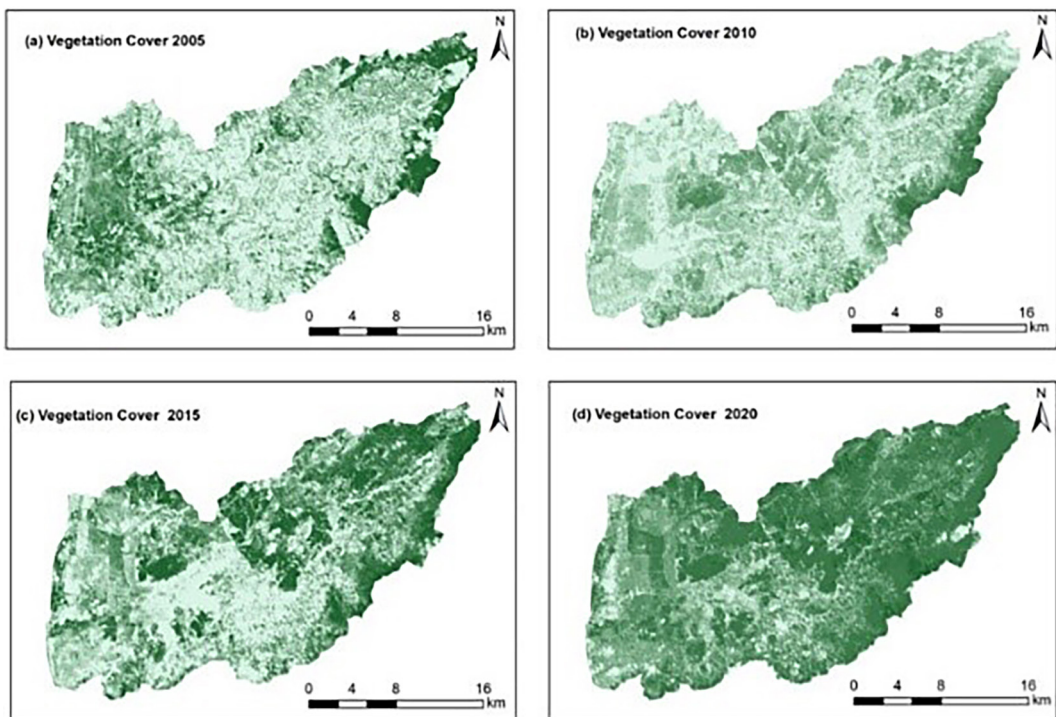


Figure 5. Distribution of vegetation cover in Tabunio watershed 2005–2020

**Table 2.** Vegetation density class of Tabunio Watershed in 2005–2020

No.	Vegetation density	2005		2010		2015		2020	
		Area [ha]	[%]						
1	Non-vegetation	22,042.56	31.22	25,383.23	36.56	13,818.00	28.07	6,604.85	10.56
2	Very sparse vegetation	8,956.65	14.32	13,025.18	20.82	8,207.37	13.12	5,974.46	9.55
3	Sparse vegetation	7,432.07	11.88	8,279.01	13.23	7,214.35	11.53	9,831.04	15.71
4	Dense vegetation	15,566.11	8.90	14,360.51	6.97	17,309.85	26.68	13,914.06	22.24
5	Very dense vegetation	8,561.17	13.69	1,510.63	2.41	16,008.99	25.59	26,234.16	41.94

of plantation land in 2005 caused a lot of non-vegetated land, which gradually changed in the following year period along with plant growth. At the end of 2020, the percentage of very dense vegetation became increasingly dominant, which was around 42 percent, as observed in Table 2.

The three biophysical indices (NDVI, SI, and BI) used in the FCD approach were appropriate for precisely discriminating between all canopy density classes, as seen by the overall producer's accuracy of 81.3%. An improved categorization results from the selective separation of the soil reflectivity component a crucial spatial feature of the Tabunio Watershed landscape from the current canopy cover using the FCD model. Conversely, locations with high SI values and seemingly dark soil (indicating low irradiant data) could be mistakenly identified as lush vegetation rather than bare land. Combining the SI and the BI solves this problem when utilizing the FCD model. This approach enables the identification of black soil conditions, hence avoiding misclassifications when both the soil index (SI) and biological index (BI) are elevated at the same site. The FCD technique effectively addresses the intricate reflectance of plants by integrating biophysical information into its computational framework. Nevertheless, we acquired a little reduced producer's accuracy for the sparse vegetation category. This outcome may indicate some of the constraints associated with employing this methodology in tropical vegetation that is exceedingly sparse. The existence of bare soil surfaces with a high level of reflectans in these regions is a result of the scarcity of water resources, which may dominate the smaller element that is indicated by very sparse vegetation. Sparse vegetation represents a sparser type than dense vegetation and very dense vegetation, as evidenced by the forest canopy density range of. Consequently, the bare soil component exhibits a much higher reflectivity in the very sparse vegetation class than in the dense and very dense classes.

As a result, the spectral separation of very sparse vegetation and non vegetation in tropical regions is characterized by a comparatively low level of accuracy, as it is observed in regions with low forest canopy density. Furthermore, it has been previously acknowledged that the FCD model may have certain constraints, as it necessitates an understanding of ground conditions to establish threshold values [Fahmi et al., 2023; Nugraha & Citra, 2020]. In general, the FCD model exhibited outstanding accuracy and strong agreement (OA = 78.0%; K = 0.71), resulting in well rounded estimates of the forest canopy density in the Tabunio Watershed. The FCD method is also helpful for the application of MRV [Monitoring, Reporting, and Verification]. The advantage of the FCD model is that it calculates the forest canopy density, not only considering the vegetation factor but also temperature and bare soil, which are negatively correlated to vegetation [Godinho et al., 2016]. The FCD model employs vegetation cover density as a crucial methods for describing forest conditions over a period of time [Fahmi et al., 2023].

## CONCLUSIONS

According to the conducted research, it can be inferred that the vegetation coverage in the Tabunio Watershed exhibited a general pattern of being high in the northeastern and eastern regions, while low in practically all areas of the western region. The state of the vegetation cover in the Tabunio watershed from 2005 to 2010 is dominated by class non vegetation and dense vegetation. At the end of 2015 until 2020 the percentage of very dense vegetation becomes increasingly dominant, which is around 42 percent. Changes in vegetation cover over two decades are very significant. The expansion of plantation land in 2005 caused a lot of non-vegetated land, which gradually changed in the following year period along

with plant growth. The study's findings suggest that the FCD model used in this research is highly effective in identifying the visible area's surface characteristics. FCD model can provide more accurate estimates of forest density compared to conventional methods. In addition, it can detect small changes in forest cover that may be missed by other models. This helps in the early identification of deforestation or forest degradation activities, and effective for forest management and conservation planning.

### Acknowledgement

The funding for this study was provided by National Competitive Applied Research Grant of The Ministry of Education, Culture, Research, and Technology [026/E5/PG.02.00.PL/2023]. The authors express their gratitude to the anonymous reviewers for their constructive feedback on previous versions of this paper.

### REFERENCES

- Amiri, R., Weng, Q., Alimohammadi, A., Alavipanah, S.K. 2009. Spatial-temporal dynamics of land surface temperature in relation to fractional vegetation cover and land use/cover in the Tabriz urban area, Iran. *Remote Sensing of Environment*, 113(12), 2606–2617. <https://doi.org/10.1016/j.rse.2009.07.021>
- Aires, U.R.V., da Silva, D.D., Moreira, M.C., Ribeiro, C.A.A.S., Ribeiro, C.B. de M. 2020. The Use of the Normalized Difference Vegetation Index to Analyze the Influence of Vegetation Cover Changes on the Streamflow in the Manhuaçu River Basin, Brazil. *Water Resources Management*, 34(6), 1933–1949. <https://doi.org/10.1007/s11269-020-02536-1>
- Auliana, A., Ridwan, I., Nurlina, N. 2018. Analisis Tingkat Kekritisan Lahan di DAS Tabunio Kabupaten Tanah Laut. *Positron*, 7(2), 54. <https://doi.org/10.26418/positron.v7i2.18671>
- Baloloy, A.B., Blanco, A.C., Raymund Rhommel, R.R.C., Nadaoka, K. 2020. Development and application of a new mangrove vegetation index (MVI) for rapid and accurate mangrove mapping. *ISPRS Journal of Photogrammetry and Remote Sensing*, 166(January), 95–117. <https://doi.org/10.1016/j.isprsjprs.2020.06.001>
- Ben Abbes, A., Bounouh, O., Farah, I.R., de Jong, R., Martínez, B. 2018. Comparative study of three satellite image time-series decomposition methods for vegetation change detection. *European Journal of Remote Sensing*, 51(1), 607–615. <https://doi.org/10.1080/22797254.2018.1465360>
- Carbajal-Morán, H., Márquez-Camarena, J.F., Galván-Maldonado, C.A., Zárate-Quiñones, R.H., Galván-Maldonado, A.C., Muñoz-De la Torre, R.J. 2023. Evaluation of Normalized Difference Vegetation Index by Remote Sensing with Landsat Satellites in the Tayacaja Valley in the Central Andes of Peru. *Ecological Engineering and Environmental Technology*, 24(7), 208–215. <https://doi.org/10.12912/27197050/169530>
- Clevers, J.G.P. W., Kooistra, L., van den Brande, M.M.M. 2017. Using Sentinel-2 data for retrieving LAI and leaf and canopy chlorophyll content of a potato crop. *Remote Sensing*, 9(5), 1–15. <https://doi.org/10.3390/rs9050405>
- Durigon, V.L., Carvalho, D.F., Antunes, M.A.H., Oliveira, P.T.S., Fernandes, M.M. 2014. NDVI time series for monitoring RUSLE cover management factor in a tropical watershed. *International Journal of Remote Sensing*, 35(2), 441–453. <https://doi.org/10.1080/01431161.2013.871081>
- Ejegu, M.A., Reta, K.G., Yegizaw, E.S., Biru, B.Z., Mekonnen, D.M., Wassie, G.K., Tegegne, M.A., Dirar, T.M., Dubale, Y.G. 2022. Land management, dynamics and vegetation vulnerability analysis in the Guna-Tana watershed as a predictor of land degradation, using remote sensing data. *Journal of Degraded and Mining Lands Management*, 9(4), 3703. <https://doi.org/10.15243/jdmlm.2022.094.3703>
- Fahmi, S., Somantri, L., Ridwana, R. 2023. Pemanfaatan Citra Sentinel-2a Multi Temporal Untuk Monitoring Perubahan Kanopi Hutan Kecamatan Belinyu Kabupaten Bangka Menggunakan Analisis Forest Canopy Density. *Jurnal Hutan Tropis*, 11(3), 380. <https://doi.org/10.20527/jht.v11i3.17633>
- Fang, H., Li, S., Zhang, Y., Wei, S., Wang, Y. 2021. New insights of global vegetation structural properties through an analysis of canopy clumping index, fractional vegetation cover, and leaf area index. *Science of Remote Sensing*, 4(May), 100027. <https://doi.org/10.1016/j.srs.2021.100027>
- Gandhi, G.M., Parthiban, S., Thummalu, N., Christy, A. 2015. Ndvi: Vegetation Change Detection Using Remote Sensing and Gis - A Case Study of Vellore District. *Procedia Computer Science*, 57, 1199–1210. <https://doi.org/10.1016/j.procs.2015.07.415>
- Gao, L., Wang, X., Johnson, B.A., Tian, Q., Wang, Y., Verrelst, J., Mu, X., Gu, X. 2020. Remote sensing algorithms for estimation of fractional vegetation cover using pure vegetation index values: A review. *ISPRS Journal of Photogrammetry and Remote Sensing*, 159(November 2019), 364–377. <https://doi.org/10.1016/j.isprsjprs.2019.11.018>
- Gupta, K., Mukhopadhyay, A., Giri, S., Chanda, A., Datta Majumdar, S., Samanta, S., Mitra, D., Samal, R.N., Pattnaik, A.K., Hazra, S. 2018. An index for discrimination of mangroves from

- non-mangroves using LANDSAT 8 OLI imagery. *MethodsX*, 5, 1129–1139. <https://doi.org/10.1016/j.mex.2018.09.011>
15. Ghosh, S.M., Behera, M.D., Jagadish, B., Das, A.K., Mishra, D.R. 2021. A novel approach for estimation of aboveground biomass of a carbon-rich mangrove site in India. *Journal of Environmental Management*, 292. <https://doi.org/10.1016/j.jenvman.2021.112816>
  16. Godinho, S., Gil, A., Guiomar, N., Neves, N., Pinto-Correia, T. 2016. A remote sensing-based approach to estimating montado canopy density using the FCD model: a contribution to identifying HNV farmlands in southern Portugal. *Agroforestry Systems*, 90(1), 23–34. <https://doi.org/10.1007/s10457-014-9769-3>
  17. Guha, S., Govil, H. 2021. An assessment on the relationship between land surface temperature and normalized difference vegetation index. *Environment, Development and Sustainability*, 23(2), 1944–1963. <https://doi.org/10.1007/s10668-020-00657-6>
  18. Guo, J., Wang, K., Wang, T., Bai, N., Zhang, H., Cao, Y., Liu, H. 2022. Spatiotemporal Variation of Vegetation NDVI and Its Climatic Driving Forces in Global Land Surface. *Polish Journal of Environmental Studies*, 31(4), 3541–3549. <https://doi.org/10.15244/pjoes/147194>
  19. Huang, S., Tang, L., Hupy, J.P., Wang, Y., Shao, G. 2021. A commentary review on the use of normalized difference vegetation index (NDVI) in the era of popular remote sensing. *Journal of Forestry Research*, 32(1), 1–6. <https://doi.org/10.1007/s11676-020-01155-1>
  20. Hussain, N., Islam, M.N. 2020. Hot spot (Gi\*) model for forest vulnerability assessment: a remote sensing-based geo-statistical investigation of the Sundarbans mangrove forest, Bangladesh. *Modeling Earth Systems and Environment*, 6(4), 2141–2151. <https://doi.org/10.1007/s40808-020-00828-4>
  21. Huylenbroeck, L., Laslier, M., Dufour, S., Georges, B., Lejeune, P., Michez, A. 2020. Using remote sensing to characterize riparian vegetation: A review of available tools and perspectives for managers. *Journal of Environmental Management*, 267(December 2019), 110652. <https://doi.org/10.1016/j.jenvman.2020.110652>
  22. Jia, M., Wang, Z., Wang, C., Mao, D., Zhang, Y. 2019. A new vegetation index to detect periodically submerged mangrove forest using single-tide Sentinel-2 imagery. *Remote Sensing*, 11(17), 1–17. <https://doi.org/10.3390/rs11172043>
  23. Kadir, S., Badaruddin, Nurlina, Ridwan, I., Rianawaty, F. 2016. The recovery of tabunio watershed through enrichment planting using ecologically and economically valuable species in south Kalimantan, Indonesia. *Biodiversitas*, 17(1), 140–147. <https://doi.org/10.13057/biodiv/d170121>
  24. Li, F., Chen, W., Zeng, Y., Zhao, Q., Wu, B. 2014. Improving estimates of grassland fractional vegetation cover based on a pixel dichotomy model: A case study in Inner Mongolia, China. *Remote Sensing*, 6(6), 4705–4722. <https://doi.org/10.3390/rs6064705>
  25. Li, M., Zang, S., Zhang, B., Li, S., Wu, C. 2014. A review of remote sensing image classification techniques: The role of Spatio-contextual information. *European Journal of Remote Sensing*, 47(1), 389–411. <https://doi.org/10.5721/EuJRS20144723>
  26. Loi, D.T., Chou, T.-Y., Fang, Y.-M. 2017. Integration of GIS and Remote Sensing for Evaluating Forest Canopy Density Index in Thai Nguyen Province, Vietnam. *International Journal of Environmental Science and Development*, 8(8), 539–542. <https://doi.org/10.18178/ijesd.2017.8.8.1012>
  27. Long, X., Li, X., Lin, H., Zhang, M. 2021. Mapping the vegetation distribution and dynamics of a wetland using adaptive-stacking and Google Earth Engine based on multi-source remote sensing data. *International Journal of Applied Earth Observation and Geoinformation*, 102, 102453. <https://doi.org/10.1016/j.jag.2021.102453>
  28. Mazzarino, M., Finn, J.T. 2016. An NDVI analysis of vegetation trends in an Andean watershed. *Wetlands Ecology and Management*, 24(6), 623–640. <https://doi.org/10.1007/s11273-016-9492-0>
  29. Ministry of Forestry Directorate of Watershed Management and Social Forestry. Barito River Watershed Management Center. 2013. Report on the Preparation of Baseline Data of Tabunio Watershed Management Ds. Banjarbaru.
  30. Mu, X., Song, W., Gao, Z., McVicar, T.R., Donohue, R.J., Yan, G. 2018. Fractional vegetation cover estimation by using multi-angle vegetation index. *Remote Sensing of Environment*, 216(June), 44–56. <https://doi.org/10.1016/j.rse.2018.06.022>
  31. Nugraha, A.S.A., Citra, I.P.A. 2020. Modifikasi Model Forest Canopy Density ( Fcd ) Pada Citra Landsat 8 Multitemporal Untuk Monitoring Perubahan Tutupan Vegetasi Di Kecamatan Sukasada-Bali. *Jurnal Penginderaan Jauh*, 17(2), 149–159. <https://doi.org/http://dx.doi.org/10.30536/j.pjpdcd.2020.v17.a3380>
  32. Nurlina, Kadir, S., Kurnain, A., Ilham, W., Kalimantan, S., Kalimantan, S., Kalimantan, S., Program, P.S. 2021. Comparison of Maximum Likelihood and Support Vector Machine Classifiers For Land Use/Land Cover Mapping Using Multitemporal Imagery. 12(June), 126–139. [http://www.savap.org.pk/journals/ARInt./Vol.12\(1\)/ARInt.2021\(12.1-12\).pdf](http://www.savap.org.pk/journals/ARInt./Vol.12(1)/ARInt.2021(12.1-12).pdf)
  33. Nurlina, Kadir, S., Kurnain, A., Ilham, W., Ridwan, I. 2022. Analysis of soil erosion and its relationships with land use/cover in Tabunio watershed. *IOP Conference Series: Earth and Environmental Science*, 976(1), 012027. <https://doi.org/10.1088/1755-1315/976/1/012027>

34. Nurlina, N., Kadir, S., Kurnain, A., Ilham, W., Ridwan, I. 2023. Impact of Land Cover Changing on Wetland Surface Temperature Based on Multitemporal Remote Sensing Data. *Polish Journal of Environmental Studies*, 32(3), 2281–2291. <https://doi.org/10.15244/pjoes/157495>
35. Ouyang, W., Hao, F., Skidmore, A.K., Toxopeus, A.G. 2010. Soil erosion and sediment yield and their relationships with vegetation cover in upper stream of the Yellow River. *Science of the Total Environment*, 409(2), 396–403. <https://doi.org/10.1016/j.scitotenv.2010.10.020>
36. Richards, D.R., Belcher, R.N. 2020. Global changes in urban vegetation cover. *Remote Sensing*, 12(1). <https://doi.org/10.3390/RS12010023>
37. Ridwan, I., Kadir, S., Nurlina, N. 2024. Wetland degradation monitoring using multi-temporal remote sensing data and watershed land degradation index. *Global Journal of Environmental Science and Management*, 10(1), 83–96. <https://doi.org/10.22034/gjesm.2024.01.07>
38. Samanta, S., Hazra, S., Mondal, P.P., Chanda, A., Giri, S., French, J.R., Nicholls, R.J. 2021. Assessment and attribution of mangrove forest changes in the indian sundarbans from 2000 to 2020. *Remote Sensing*, 13(24). <https://doi.org/10.3390/rs13244957>
39. Sahana, M., Sajjad, H., Ahmed, R. 2015. Assessing spatio-temporal health of forest cover using forest canopy density model and forest fragmentation approach in Sundarban reserve forest, India. *Modeling Earth Systems and Environment*, 1(4), 1–10. <https://doi.org/10.1007/s40808-015-0043-0>
40. Song, W., Mu, X., Ruan, G., Gao, Z., Li, L., Yan, G. 2017. Estimating fractional vegetation cover and the vegetation index of bare soil and highly dense vegetation with a physically based method. *International Journal of Applied Earth Observation and Geoinformation*, 58, 168–176. <https://doi.org/10.1016/j.jag.2017.01.015>
41. Song, Y., Jin, L., Wang, H. 2018. Vegetation changes along the Qinghai-Tibet Plateau Engineering Corridor since 2000 induced by climate change and human activities. *Remote Sensing*, 10(1), 1–21. <https://doi.org/10.3390/rs10010095>
42. Sun, H., Wang, J., Xiong, J., Bian, J., Jin, H., Cheng, W., Li, A. 2021. Vegetation Change and Its Response to Climate Change in Yunnan Province, China. *Advances in Meteorology*, 2021. <https://doi.org/10.1155/2021/8857589>
43. Tian, J., Yue, J., Philpot, W.D., Dong, X., Tian, Q. 2021. Soil moisture content estimate with drying process segmentation using shortwave infrared bands. *Remote Sensing of Environment*, 263(June), 112552. <https://doi.org/10.1016/j.rse.2021.112552>
44. Vaghela, B.N., Parmar, M.G., Solanki, H.A., Kansara, B.B., Prajapati, S.K., Kalubarme Editors Cem Gazioğlu, M.H., Zafer Şeker, D., Tanık, A., Kaya, Ş., Volkan Demir, A., Aksu, A., Alpar, B., Altuğ, G., Balas, L., Balas, C., Bat, L., Bayram, B., Çağlar, N., Dash, J., Kalubarme, M.H. 2018. Multi Criteria Decision Making (MCDM) Approach for Mangrove Health Assessment using Geo-informatics Technology. *International Journal of Environment and Geoinformatics*, 5(2), 114–131. <https://doi.org/10.30897/ijegeo>
45. Wibawa, D.T., Fithria, A., Nisa, K. 2021. Perubahan Penutupan Lahan Di Das Tabunio, Kabupaten Tanah Laut, Kalimantan Selatan. *Jurnal Sylva Scientae*, 4(1), 59. <https://doi.org/10.20527/jss.v4i1.3093>
46. Yan, K., Gao, S., Chi, H., Qi, J., Song, W., Tong, Y., Mu, X., Yan, G. 2022. Evaluation of the Vegetation-Index-Based Dimidiate Pixel Model for Fractional Vegetation Cover Estimation. *IEEE Transactions on Geoscience and Remote Sensing*, 60, 1–14. <https://doi.org/10.1109/TGRS.2020.3048493>
47. Zaitunah, A., Samsuri, S., Ahmad, A.G., Safitri, R.A. 2018. Normalized difference vegetation index (ndvi) analysis for land cover types using landsat 8 oli in besitang watershed, Indonesia. *IOP Conference Series: Earth and Environmental Science*, 126(1). <https://doi.org/10.1088/1755-1315/126/1/012112>